Thin Solid Films 519 (2011) 7458–7463

Contents lists available at ScienceDirect

Thin Solid Films

journal homepage: www.elsevier.com/locate/tsf

Rocking disc electro-deposition of copper films on Mo/$MoSe_2$ substrates

Charles Y. Cummings [a], Paul E. Frith [a], Guillaume Zoppi [b], Ian Forbes [b], Keith D. Rogers [c], David W. Lane [d], Frank Marken [a,*]

[a] Department of Chemistry, University of Bath, Claverton Down, Bath BA2 7AY, UK
[b] Northumbria Photovoltaics Applications Centre, Northumbria University, NE1 8ST, UK
[c] Cranfield Health, Cranfield University, Shrivenham Campus, Swindon, SN6 8LA, UK
[d] Department of Applied Science, Security and Resilience, Cranfield University, Shrivenham, Swindon, SN6 8LA, UK

ARTICLE INFO

Available online 25 December 2010

Keywords:
Voltammetry
Turbulence
Diffusion
Electro-deposition
Copper
Molybdenum
Selenide
Electrochemistry
Solar cell
Photovoltaics

ABSTRACT

A novel electro-deposition method based on a rocking disc system with π/3 amplitude and variable frequency is introduced. Uniform copper films were deposited from a 0.1 M $CuSO_4$/3.0 M NaOH/0.2 M sorbitol bath directly onto 12.1 cm^2 Mo/$MoSe_2$ substrates with X-ray diffraction showing a thickness variation of ±5% over this area. Investigation of the mass transport conditions suggests (i) uniform diffusion over the sample, (ii) a rate of mass transport proportional to the square root of the rocking rate, and (iii) turbulent conditions, which are able to dislodge gas bubbles during electro-deposition.

1. Introduction

Electro-deposition is a widely used and commercially beneficial technology with applications in producing films and coatings of metals and alloys [1], semiconductors [2,3], and more specifically photovoltaic absorber layers [4,5]. Electro-deposition allows high throughput, wet environments, use of non-ideal (non-planar) substrates, and thickness/composition control by external parameters such as the applied potential and mass transport [6]. In order to form uniformly thick electro-deposits, both the applied potential and mass transport must remain constant spatially over the working electrode and in time. A commonly employed tool for the control of mass transport is rotating disc electro-deposition where the working electrode is rotated uniformly to generate a hydrodynamic flow profile with close to uniform and constant rate of diffusion to the electrode surface [7]. Rotating disc techniques have been routinely employed in electro-deposition of thin film semiconductor absorber layers [8] with typically up to 4 cm^2 area, but the method suffers from severe technical problems when larger electrode surfaces need to be coated.

Here, we introduce a novel technique, rocking disc electro-deposition, where the working electrode (area 12.1 cm^2) is placed at the cell bottom, a counter electrode is positioned at the cell lid symmetrically opposing the working electrode, a reference electrode is placed into the center in close distance to the working electrode, and a rocking movement (π/3) introduces a turbulent but uniform flow across the working electrode. It is shown that uniform mass transport conditions are achieved at sufficiently high rocking rates and that uniform copper films can be electro-deposited.

2. Experimental methods

2.1. Reagents

Sodium hydroxide (97%), D-sorbitol (98%), potassium chloride (98%), and hexaammine ruthenium(III) chloride (99.9+%) were obtained from Sigma-Aldrich and used without further purification. Copper(II) sulphate (A.C.S. grade) was purchased from Alfa Aesar. Solutions were prepared in demineralized and filtered water taken from a Thermo Scientific water purification system (Barnstead Nanopure) with 18.2 MΩcm resistivity.

2.2. Instrumentation

For voltammetry studies, a microAutolab II potentiostat system (EcoChemie, Netherlands) was employed with a KCl-saturated calomel reference electrode (SCE, Radiometer). For all experiments, the reference electrode was placed centrally in approximately 2 mm distance from the working electrode. The counter electrode was positioned at the top of the cylindrical cell (Fig. 1B) and was

* Corresponding author. Tel.: +44 1225 383694; fax: +44 1225 386231.
E-mail address: F.Marken@bath.ac.uk (F. Marken).

0040-6090/$ – see front matter © 2010 Elsevier B.V. All rights reserved.
doi:10.1016/j.tsf.2010.12.107

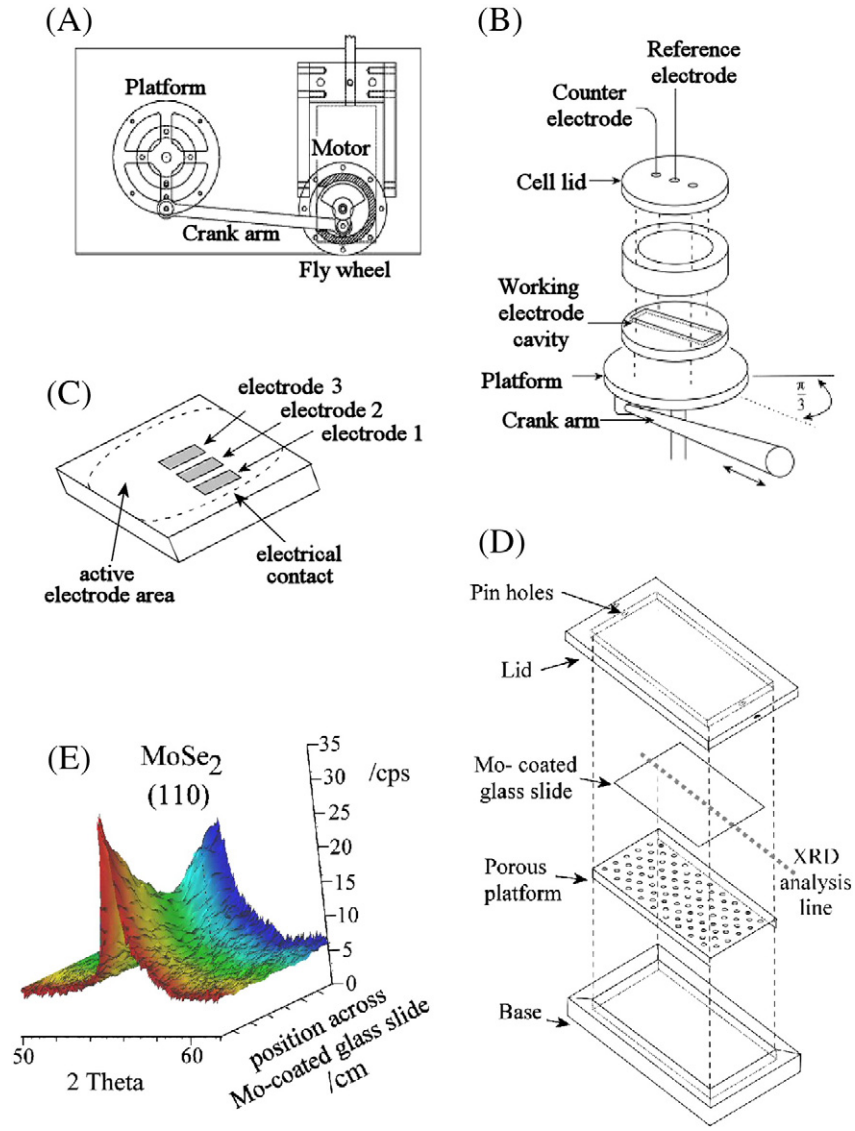

Fig. 1. (A) Schematic drawing of the rocking disc voltammetry system with an electrochemical cell mounted on a rocking platform. (B) The 45 cm^3 electrochemical cell consists of a working electrode inlaid at the bottom of the cell with a central reference in ca. 2 mm distance and a counter electrode disc (copper) embedded into the cell lid. (C) The working electrode is a glass slide 75 mm × 26.5 mm with a central circular region exposed to the electrolyte solution. A calibration electrode with three gold working electrodes (area 5 mm × 5 mm; 5 mm gap; with electrode 3 in the center and electrode 1 placed 3 mm from the cell wall) was employed to determine local mass transport conditions. (D) Schematic drawing of the carbon selenization box, which was charged with 15 mg Se in the bottom and placed into a flow of N_2 in a furnace. The Mo-coated glass slide is placed face-up on a porous platform to react with the selenium vapor predominantly at the front and end. (E) XRD of 110 $MoSe_2$ diffraction line as a function of position across the Mo/$MoSe_2$ electrode substrate (see dashed line in A).

composed of a sheet of metallic copper (Advent 99.99%) with dimensions 2 mm × 50 mm × 50 mm. In voltammetry experiments exploring mass transport during vibration, the working electrode was a glass slide (75 mm × 26.5 mm) with three individual gold electrodes (5 mm × 5 mm) evaporated onto the surface (Fig. 1C). For plating experiments Mo/$MoSe_2$ film electrodes [9] deposited on a glass slide (75 mm × 26.5 mm) were employed. Electrochemical experiments using solutions containing hexaammine ruthenium(III) chloride were conducted in de-aerated solution (BOC Pureshield argon). The electro-deposition of copper was conducted in ambient atmosphere. The temperature for all experiments was 22 ± 2 °C.

The surface morphology and topology of the films were observed using a JEOL JSM6480LV scanning electron microscope (SEM). X-ray diffraction analysis was carried out using a PANalytical X'Pert PRO Multi-Purpose diffractometer with Cu Kα radiation and a PIXcel detector.

2.3. Design and operation of the rocking disc hydrodynamic electro-deposition system

The electro-deposition system consists of the electrochemical cell mounted on a freely rotating platform (Fig. 1A) connected with a fly wheel (linked to an IKA Eurostar digital motor) using a crank arm. The electro-deposition cell is a hollow poly-carbonate cylinder with external dimensions (height is 38 mm and radius is 57 mm) and internal dimensions (height is 21 mm and radius is 25 mm).

2.4. Formation and characterization of Mo/$MoSe_2$ film electrodes

Mo working electrodes were made with an approximately 0.8 μm thick film of metallic Mo RF-sputtered onto soda-lime glass slides (75 mm × 26.5 mm). The selenization of the Mo-coated glass slides was reported previously [9] and briefly, it was performed by placing a clean

Mo-coated glass slide (sonicated in Decon 90 and in 5% w/w and ethanol, both 1 min, drying under nitrogen) face-up in a custom-made carbon box (with a width to fit the slide and a length of ca. 100 mm) charged with 15 mg of elemental selenium. The box was placed in a selenization tube furnace, evacuated, and filled with nitrogen. Selenization took place under flow of nitrogen (10 $cm^3\,min^{-1}$) and by heating to 500 °C (ramp rate 10 °C min^{-1}) and holding 500 °C for 1 h. The chamber was then cooled to room temperature at −1 °C min^{-1}. Electrical contact to the underling Mo film was possible by gently removing part of the ca. 0.1 μm thick $MoSe_2$ layer (with a cotton bud) and adhering a Cu wire (Advent 99.99%) using silver epoxy (RS). The exposed area of the working electrode was 12.1 cm^2.

In XRD analysis of the Mo/$MoSe_2$ film electrodes, both Mo and $MoSe_2$ crystalline phases are observed. The $MoSe_2$ 110 diffraction maxima are shown in Fig. 1E as a function of position along the Mo/$MoSe_2$ electrode. Relatively large widths at half peak heights are observed for the $MoSe_2$ reflections, presumably because of a significant amount of lattice disorder. From the peak height versus position, it is apparent that the selenization of molybdenum does not create completely uniform $MoSe_2$ thin films. The 110 reflections are higher at either end of the electrode possibly due to a thickness and/or crystal morphology gradient caused by a selenium vapor pressure gradient from the sample edge to the center during selenization (see Fig. 1D). However, the electrical conductivity of the $MoSe_2$ film is high and the thickness/morphological gradient does not affect the electrochemical processes.

2.5. Cu plating procedure

For the electro-deposition of metallic copper, a non-cyanide, highly alkaline plating bath was used. As proposed by Barbosa et al. [10], the copper plating solution contained 3.0 M sodium hydroxide and 0.2 M D-sorbitol, and either 0.01 M (for voltammetry) or 0.1 M (for plating) copper sulphate was employed. Using this solution, copper was electroplated onto Mo/$MoSe_2$ electrode substrates for a pre-defined charge with the rocking disc electro-deposition system.

3. Results and discussion

3.1. Rocking disc voltammetry I: reduction of $Ru(NH_3)_6^{3+}$ at gold array electrodes

In order to explore mass transport conditions during rocking disc voltammetry, the $Ru(NH_3)_6^{3+/2+}$ redox system is employed as a well-known reversible one-electron reduction (see Eq. (1)).

$$Ru(NH_3)_6^{3+}(aq) + e^- \rightleftharpoons Ru(NH_3)_6^{2+}(aq) \quad (1)$$

Typical voltammetric responses are shown in Fig. 2A. The reversible $Ru(NH_3)_6^{3+/2+}$ redox system is observed at ca. −0.18 V vs. SCE [11]. In the absence of agitation, identical voltammograms are observed at gold electrodes 1, 2, and 3 (see Fig. 1C). The effect of rocking motion of the electrochemical cell on the electrochemical process is clearly observed as an increase in reduction current and a change in shape from a typical transient voltammogram (see Fig. 2A curve i) to a steady-state voltammogram (see Fig. 2A curve v). Fig. 2B demonstrates the corresponding transition as a function of scan rate. For a high rocking rate (16.7 s^{-1}), the limiting current exhibits some superimposed noise due to the turbulent flow induced under these conditions, but also a well-defined steady-state limiting current response is observed similar to that observed under rotating disc conditions [12]. Furthermore, a comparison of current responses at electrode 1 (at the outer limit of the working electrode area), electrode 2 (in the middle), and electrode 3 (in the center of the electrochemical cell, see Fig. 1C) suggests insignificant differences and essentially identical limiting currents as a function of rocking rate. This result is important because it implies a uniform current density and therefore good electro-plating conditions. A plot of the limiting (or peak) current versus rocking rate is shown in Fig. 2C. Under steady-state conditions (with a rocking rate higher than 2 s^{-1}), a linear dependence of limiting current on the square root of the rocking rate is observed empirically. This result suggests that in spite of the complex π/3-rocking motion, conditions at the electrode surface are similar to those under rotating disc voltammetry conditions. The limiting current, $I_{lim} = 120$ μA, observed at a 16.7 s^{-1} rocking rate can be translated into an average diffusion layer thickness δ based on Eq. (2).

$$\delta = \frac{nFDAc}{I_{lim}} \quad (2)$$

In this equation the average diffusion layer thickness δ is given by *n*, the number of electrons transferred per molecule diffusion to the electrode, *F*, the Faraday constant, *D*, the diffusion coefficient (here $0.9\times10^{-9}\ m^2s^{-1}$ [13]), *A*, the electrode area, *c*, the bulk concentration of the redox active component, and I_{lim}, the observed limiting current. At a rocking rate of 16.7 s^{-1}, the average diffusion layer thickness is δ = 18 μm. This rocking rate can be compared with a corresponding rotation rate for a rotating disc voltammetry experiment (see Eq. (3) [14]) of 11.8 s^{-1}.

$$\delta_{RDE} = \frac{D^{1/3}\nu^{1/6}}{0.62\sqrt{2\pi f}} \quad (3)$$

In this equation, δ_{RDE} is the diffusion layer thickness at a rotating disc electrode, *v* denotes the kinematic viscosity, and *f* is the rate of revolution in s^{-1}. The similarity in values for rocking rate and rate of revolution suggests similar conditions apart from the fact that under rocking disc voltammetry conditions a more turbulent flow occurs. The rocking amplitude (here π/3) is an important parameter, which could allow further adjustment of the rate of mass transport. Table 1A summarizes the voltammetry data for the reduction of $Ru(NH_3)_6^{3+}$ at gold electrodes in positions 1, 2, and 3 as a function of rocking rate.

In order to further investigate the flow conditions within the rocking electrochemical cell, generator–collector experiments are carried out where one electrode is employed to "generate" a reduction product and a second electrode is "collecting". No significant collector currents were observed up to 16.7 s^{-1} rocking rate when electrode 3 was used. However, currents are observed when electrode 2 is the generator and electrode 1 is the collector. Fig. 2D shows typical cyclic voltammograms for the one-electron reduction of 1 mM $Ru(NH_3)_6^{3+}$ in aqueous 0.1 M KCl at electrode 2 and re-oxidation at electrode 1. With a 8.3 s^{-1} rocking rate well-defined limiting currents are observed and the collector response shows hysteresis due to the delay of $Ru(NH_3)_6^{2+}$ being transported between the two electrodes. Fig. 2E shows a plot of generator and collector currents as a function of rocking rate. Although the hysteresis effect is changing with rocking rate, the collection efficiency $\left(=\frac{I_{lim}(\text{collector})}{I_{lim}(\text{generator})}\times 100\%\right)$ remains at approximately 13% for rocking rates of 1.67 s^{-1} to 16.7 s^{-1}. In spite of the turbulent nature of the flow, the magnitude of this value compares well to typical collection efficiency data from rotating ring-disc electrode systems [15] and it confirms the in average radial flow pattern (see Fig. 2F). Conditions during rocking disc voltammetry are therefore suitable for thin film electro-deposition processes and two additional advantages are (i) the ability of turbulent flow to dislodge gas bubbles and (ii) the face-up orientation, which allows gas bubbles to escape.

3.2. Rocking disc voltammetry II: cyclic voltammetry and chrono-amperometry for copper electro-deposition on Mo/$MoSe_2$ electrodes

Thin copper-containing semiconductor absorber layers have been successfully developed into highly efficient solar cells [4]. The electro-deposition of copper films is part of the cost-effective CIS (copper

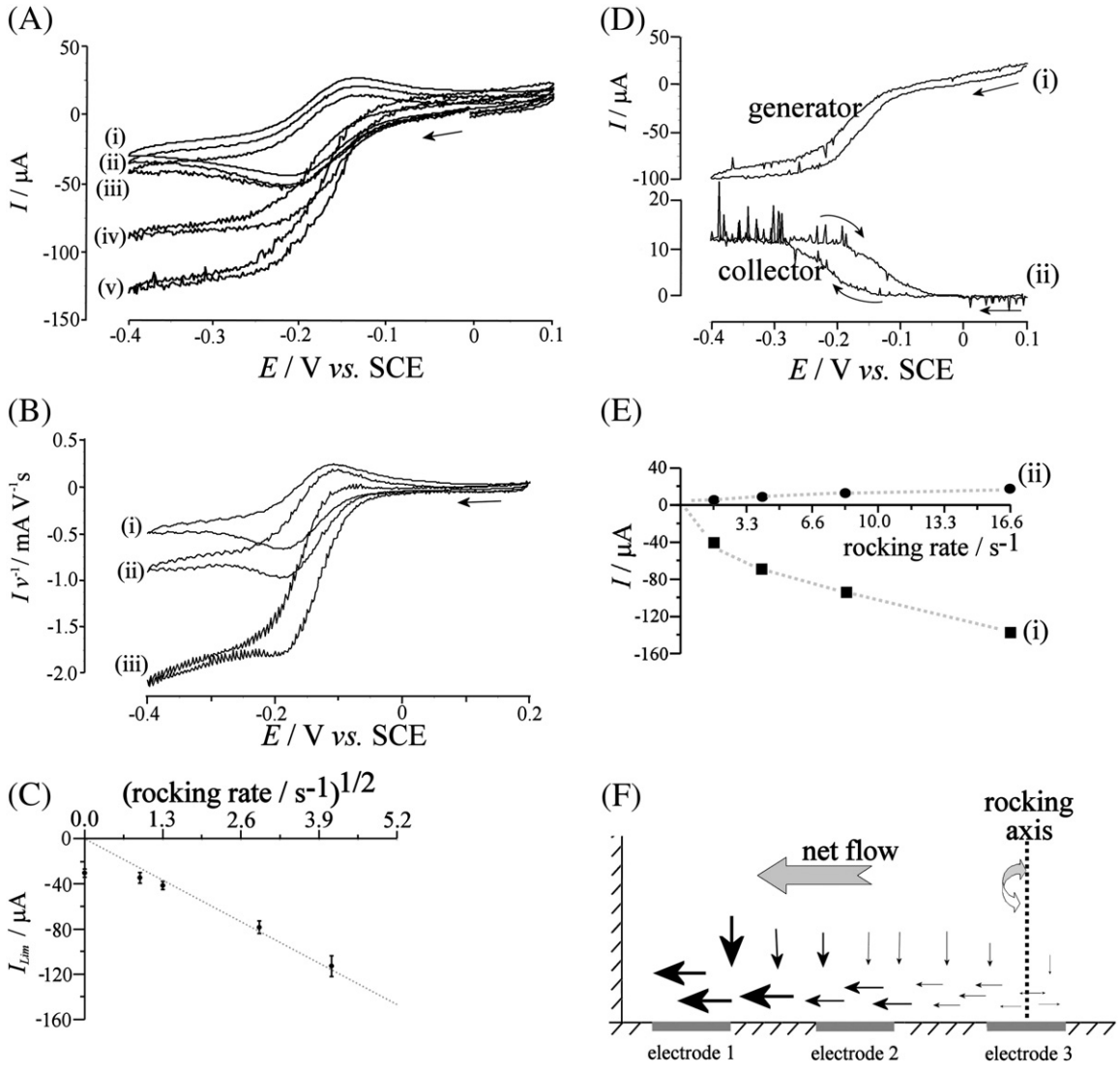

Fig. 2. (A) Cyclic voltammograms (scan rate 0.02 Vs^{-1}) for the reduction of 1 mM $Ru(NH_3)_6^{3+}$ in aqueous 0.1 M KCl at a gold electrode (electrode 3 in Fig. 1C, area 25 mm^2, located in the center of the working electrode area) obtained at rocking rates of (i) 0 s^{-1}, (ii) 0.83 s^{-1}, (iii) 1.67 s^{-1}, (iv) 8.33 s^{-1}, and (v) 16.7 s^{-1}. (B) Cyclic voltammograms as in (A) for a rocking rate of 3.3 s^{-1} and a scan rate of (i) 0.1, (ii) 0.05, and (iii) 0.02 Vs^{-1}. (C) Plot of the limiting current (the average of the limiting currents at −0.3 V vs. SCE for electrodes 1, 2, and 3) versus square root of rocking rate (error bars represent the standard deviation in current between the three electrodes). (D) Bi-potentialstatic cyclic voltammetry (rocking rate 8.3 s^{-1}, scan rate 0.02 Vs^{-1}) for the reduction of 1 mM $Ru(NH_3)_6^{3+}$ in 0.1 M KCl at electrode 2 (generator, scanning) and the re-oxidation at electrode 1 (collector, at 0.1 V vs. SCE). (E) Plot of the (i) generator and (ii) collector currents versus rocking rate. (F) Schematic drawing of the flow conditions in the rocking electrochemical cell.

indium sulphide [16]), CISe (copper indium selenide [17–20]), cuprous oxide [21], and CZTS (copper zinc tin sulphide [22]) absorber layer formation process and has been described recently for the case of Mo/$MoSe_2$ photovoltaic substrates, which are beneficial in alkaline media [9]. Fig. 3A shows a typical voltammetric response for the initial reduction of 0.1 M Cu(II). A nucleation process occurs at approximately −0.75 V vs. SCE and peaks for the reduction and stripping of copper are observed in the absence of agitation. In continuous potential cycles (see Fig. 3B), a stable voltammetric response is observed with a reversible potential of ca. −0.67 V vs. SCE. The process is likely to involve a cuprate(II) (see Eq. (4)) or possibly a sorbitol complex.

$$Cu(OH)_4^{2-} + 2e^- \rightleftharpoons Cu(metal) + 4OH^-(aq) \quad (4)$$

In the presence of rocking disc agitation, an increase in the cathodic deposition current and a change from a peak to a steady-state response are observed (Fig. 3C). The magnitude of the cathodic limiting current is I_{lim} = ca. 15 mA at 16.7 s^{-1} rocking rate and decreasing with lower rocking rate. A plot of the limiting current versus δ^{-1} (obtained from Fig. 2C) is approximately linear (not shown) suggesting mass transport control. The diffusion coefficient for the Cu(II) species can be estimated as 0.14×10^{-9} m^2s^{-1}, which is relatively low and probably an indication of the formation of a sorbitol complex. High-quality copper deposits are obtained with 0.1 M Cu(II) solution at a potential of −1.0 V vs. SCE and a typical photograph of the copper film is shown in Fig. 3D.

Copper electro-deposits obtained at 8.3 s^{-1} and at 16.7 s^{-1} were shiny and smooth (see SEM micrograph presented in Fig. 3E) and had good adhesion to the underlying Mo/$MoSe_2$ substrate. EDS counts obtained during SEM imaging (not shown) indicated uniform deposits. For thin films, XRD scans across the surface provide a sensitive tool for thickness measurements (using the diffraction peak area) and therefore XRD data were used to assess the thickness of the copper films along vertical and horizontal axes (Fig. 3F and G). Fig. 3F shows data for two reflections corresponding to the (200) and (111) lattice planes, which are both uniform. XRD data summarized in Table 1B suggest a ±5% thickness variation.

Table 1

A. Voltammetric data for the reduction of 1 mM $Ru(NH_3)_6^{3+}$ in aqueous 0.1 M KCl at a gold array electrode (see Fig. 1C) taken at −0.3 V vs. SCE and obtained as a function of rocking rate.

Rocking rate /s^{-1}	Electrode 1	Electrode 2	Electrode 3	Average
	I_{lim}/μA	I_{lim}/μA	I_{lim}/μA	I_{lim}/μA
0	−28.1	−28.1	−33.9	−31.0
0.83	−30.7	−32.5	−39.5	−36.0
1.7	−40.9	−38.0	−44.6	−41.3
8.3	−77.0	−73.4	−84.4	−78.9
16.7	−116.0	−102.0	−120.0	−111.0

B. Average XRD peak area data and standard deviation in peak area based on the sum of Cu (200) and Cu (111) XRD reflections for Cu film samples electro-deposited at 8.3 s^{-1} and 16.7 s^{-1} rocking rate.

	8.3 s^{-1}		16.7 s^{-1}	
XRD scan path (see Fig. 6E)	Average 200 and 111 peak area/a.u.	Relative standard deviation [a] in peak area/%	Average 200 and 111 peak area/a.u.	Relative standard deviation [a] in peak area/%
Vertical	7.39	5.7	6.68	10.3
Hoz. Up	7.25	2.0	6.40	2.6
Hoz. Mid	7.77	2.7	6.64	4.8
Hoz. Low	7.38	3.3	6.91	5.1

[a] Relative standard deviation calculated as the variance divided by the mean. Horizontal scans based on 25 data points and vertical scans based on 31 data points.

4. Conclusions

A new methodology of inducing uniform mass transport during electrochemical deposition in a rocking disc system is proposed and demonstrated. Benefits of this system are (i) the electrode size can be increased (here up to 12.1 cm^2) without complications in the experimental method or reproducibility, (ii) the mass transport is uniform over the electrode surface and can be controlled by changing the rocking rate, (iii) gas bubbles get dislodged and separate from the surface, and (iv) Mo/$MoSe_2$ photovoltaic substrates can be readily coated with uniform copper films with ±5% thickness variation (based on XRD scans for films deposited with 8.3 s^{-1} rocking rate) in a 0.5 μm thick film. This methodology will be of wider use for the electro-deposition of multi-layer absorber layers and for bigger wafer-sized photovoltaic substrates.

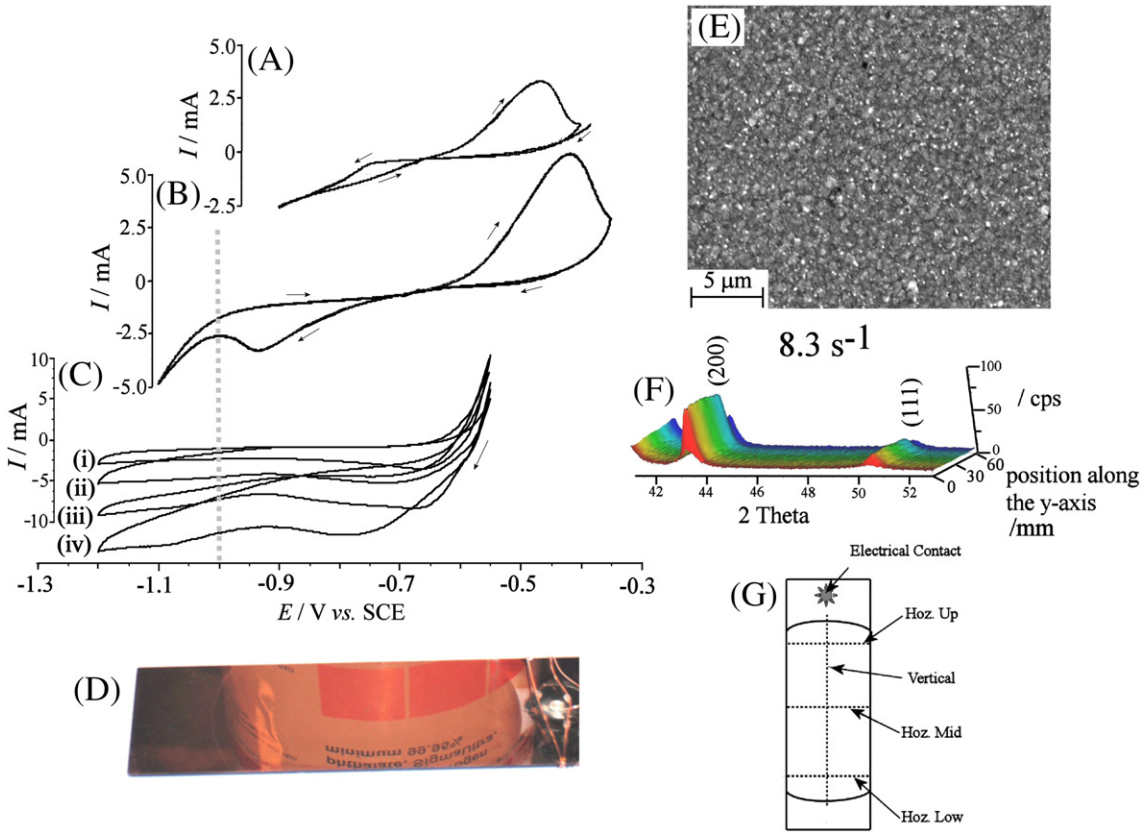

Fig. 3. (A) Cyclic voltammogram (scan rate 50 mVs^{-1}, area 1 cm^2) for the 1st potential cycle for the reduction of 0.1 M $CuSO_4$ in 3 M NaOH/0.2 M D-sorbitol at a Mo/$MoSe_2$ electrode. (B) 3rd potential cycle. (C) Cyclic voltammograms (scan rate 20 mVs^{-1}, area 10.6 cm^2, rocking rate (i) 0 s^{-1}, (ii) 0.83 s^{-1}, (iii) 8.3 s^{-1}, (iv) 16.7 s^{-1}) for the reduction of 10 mM $CuSO_4$ at a Mo/$MoSe_2$ electrode immersed in 3 M NaOH/0.2 M D-sorbitol. The dashed line indicates the electro-deposition potential of −1.0 V vs. SCE. (D) Photograph of a 14.3 C copper film (ca. 0.42 μm thick) electro-deposited onto Mo/$MoSe_2$ from 0.1 M Cu(II) at 8.3 s^{-1} rocking rate. (E) SEM image for copper films grown at −1.0 V vs. SCE with a rocking rate of 8.3 s^{-1}. (F) Plot of the XRD scans along the vertical axis for the copper films formed at rocking rates of 8.3 s^{-1}. (G) Schematic drawing of the line scan position across the working electrode.

Acknowledgments

The authors are grateful for financial support from the EPSRC (Supergen: Photovoltaic Materials for the 21st Century EP/F029624/1), for help with gold evaporation by Dr. Petra Cameron and Diego Colombara, for technical assistance during SEM imaging provided by Dr. John Mitchels, and for helpful discussion with Prof. Laurence M. Peter.

References

[1] J.W. Dini, Electrodeposition: The Materials Science of Coatings and Substrates, Noyes Publications, New York, 1992.
[2] R.K. Pandey, S.N. Sahu, S. Chandra, Handbook of Semiconductor Electrodeposition, CRC Press, New York, 1996.
[3] D. Lincot, Thin Solid Films 487 (2005) 40.
[4] D. Lincot, J.F. Guillemoles, S. Taunier, D. Guimard, J. Sicx-Kurdi, A. Chaumont, O. Roussel, O. Ramdani, C. Hubert, J.P. Fauvarque, N. Bodereau, L. Parissi, P. Panheleux, P. Fanouillere, N. Naghavi, P.P. Grand, M. Benfarah, P. Mogensen, O. Kerrec, Sol. Energy 77 (2004) 725.
[5] J.J. Scragg, D.M. Berg, P.J. Dale, J. Electroanal. Chem. 646 (2010) 52.
[6] A. Brenner, Electrodeposition of Alloys: Principles and Practice, Vol. 2, Academic Press, New York, 1963.
[7] V.G. Levich, Physicochemical Hydrodynamics, Prentice-Hall Inc., New York, 1962.
[8] M. Kurihara, D. Berg, J. Fischer, S. Siebentritt, P.J. Dale, Phys. Status Solidi C 6 (2009) 1241.
[9] C.Y. Cummings, G. Zoppi, I. Forbes, P.J. Dale, J.J. Scragg, L.M. Peter, F. Marken, J. Electroanal. Chem. 645 (2010) 16.
[10] L.L. Barbosa, M.R.H. de Almeida, R.M. Carlos, M. Yonashiro, G.M. Oliveira, I.A. Carlos, Surf. Coat. Technol. 192 (2005) 145.
[11] K.J. McKenzie, P.M. King, F. Marken, C.E. Gardner, J.V. Macpherson, J. Electroanal. Chem. 579 (2005) 267.
[12] C.M.A. Brett, A.M.O. Brett, Electrochemistry: Principles, Methods, and Applications, Oxford University Press, Oxford, 1993.
[13] F. Marken, J.C. Eklund, R.G. Compton, J. Electroanal. Chem. 395 (1995) 335.
[14] Southampton Electrochemistry Group, Instrumental Methods in Electrochemistry, Horwood, Chichester, 2004, p. 22.
[15] W.J. Albery, M.L. Hitchman, Ring-Disc Electrodes, Clarendon Press, Oxford, 1971.
[16] J. Alvarez-Garcia, B. Barcones, A. Romano-Rodriguez, L. Calvo-Barrio, A. Perez-Rodriguez, J.R. Morante, R. Scheer, R. Klenk, J. Electrochem. Soc. 150 (2003) G400.
[17] D.D. Shivagan, P.J. Dale, A.P. Samantilleke, L.M. Peter, Thin Solid Films 515 (2007) 5899.
[18] T.P. Gujar, V.R. Shinde, J.W. Park, H.K. Lee, K.D. Jung, O.S. Joo, J. Electrochem. Soc. 155 (2008) E131.
[19] O. Savadogo, Sol. Energy Mater. Sol. Cells 52 (1998) 361.
[20] M. Benaicha, N. Benouattas, C. Benazzouz, L. Ouahab, Sol. Energy Mater. Sol. Cells 93 (2009) 262.
[21] S. Joseph, P.V. Kamath, J. Electrochem. Soc. 156 (2009) E143.
[22] J.J. Scragg, P.J. Dale, L.M. Peter, G. Zoppi, I. Forbes, Phys. Status Solidi B 245 (2008) 1772.